Towards validation of the senescence-induced senescence hypothesis

Stephen Malina

1 Introduction

Cellular senescence is increasingly believed to play an important role in the aging process. Senescent cells (SnCs) are cells that can no longer divide but continue to limp along rather than actually die. In young, healthy organisms, senescent cells can play a positive role in arresting tumor growth and healing wounds (Ricón 2020; He and Sharpless 2017; Krtolica et al. 2001). However, increasing evidence points to senescent cells contributing to the aging process via slowing stem cell growth and tissue regeneration and increasing inflammation in older organisms (Campisi and Di Fagagna 2007).

A characteristic pattern that accompanies the shift in roles is an increase in relative abundance of and slowing down of turnover of senescent cells. In order to understand and intervene on cellular senescence to prolong healthy lifespan and ward off disease, we must understand the factors that drive the shift SnC growth regimes. In particular, one relative under-explored hypothesis from Nelson et al. (2012) suggests that the SnC turn over slow down may partially result from a "bystander effect" in which senescentcells induce nearby healthy cells into senescence (senescence-induced senescence, SIS).

We leveraged longitudinal and pulse data (Karin et al. 2019; Burd et al. 2013) to test how well a model that includes SIS from long-lived senescent cells captured observed senescent cell dynamics relative to two already published models (Karin et al. 2019). We also computed a point estimate and bounds on the fraction of senescent cells which our models predicted to be long-lived based on longitudinal data.

2 Methods

We built a Bayesian ODE-based model of SnC growth dynamics based on a pair of mouse SnC time-series datasets using stan (Carpenter et al. 2017). We compare our model to Bayesian versions of two previously-published models using Bayes Factors (Gronau, Singmann, and Wagenmakers 2020), Leave-One-Out Cross-Validation (LOO-CV) (Yao et al. 2017), and an extrapolation test. All of our code and data are available on Github at https://github.com/an1lam/sis.

2.1 Datasets

2.1.1 Longitudinal Dataset

Our primary dataset (originally collected by Burd et al. (2013)) measures SnC abundance in 32 mice over their entire lifespan (80 weeks, i.e. ~1.54 years). This dataset consists of total body luminescence (TBL) measurements from each mouse taken at 2 week intervals throughout each mouse's life. These luminescence measurements act as a proxy for $p16^{INK4a}$, a senescence biomarker, prevalence. $p16^{INK4a}$ itself then serves as a proxy for senescent cell prevalence throughout the body. In line with Karin et al. (2019), we preprocess unnormalized TBL values into normalized SnC abundance measurements (AUs) by dividing all luminescence values by mean luminescence during the first three weeks of the experiment (weeks 8, 16, 24).

2.1.2 Pulse Dataset

The SnC pulse dataset (from Karin et al. (2019)) measures SnC abundance in old (22 months) and young (3 months) mices' lungs after treatment with bleomycin, a compound known to induce cellular senescence a few

days after application. Similar to as with the longitudinal dataset, all SnC abundance measurements are normalized to the

2.2 Models

2.3 Bayesian Saturated Removal (SR) and Unsaturated Removal (USR) base models

As a first step towards building and assessing a model that includes senescence-induced senescence, we re-fit two existing models (Karin et al. 2019) of senescent cell growth on the longitudinal senescent cell dataset.

In their paper, Karin et al. (2019) apply a maximum likelihood framework and parameter grid search to fit 16 ODE-based models of senescent cell growth. Each of their 16 models was derived by selecting a subset of parameters from the following 'full' model of senescent cell growth with time/age,

$$\frac{\mathrm{dC}}{\mathrm{dt}} = \underbrace{(\eta_0 + \eta_1 * t)(1 + \eta_2 * C)}_{\text{production}} - \underbrace{\frac{\beta_0 - \beta_1 * t}{1 + \beta_2 * C} * C}_{\text{removal}} + \underbrace{\sqrt{2\epsilon} * \xi_t}_{\text{noise}}. \tag{1}$$

In equation (1), C denotes the normalized senescent cell abundance, measured in arbitrary units (AUs) (see Appendix for details). The first of three expression's three variables, η_0, η_1, η_2, denote initial growth rate, growth rate increase with age, and senescence-induced senescence rate respectively. The second of the three expression's three variables, $\beta_0, \beta_1, \beta_2$, denote initial removal rate, decrease in removal rate with age, and inverse of the half-way saturation point for senescent cell removal respectively. Last, the remaining term ξ_t models per time-step independent noise, which we replace with a single independent noise term.

In Karin et al. (2019), the best-performing model variant, the saturated removal (SR) model, got rid of the senescence-induced senescence term but otherwise left the model as-is. The best-performing variant without the saturated removal term (β_2), i.e. the unsaturated removal (USR) model, also excluded the senescence-induced senescence term in its growth rate expression.

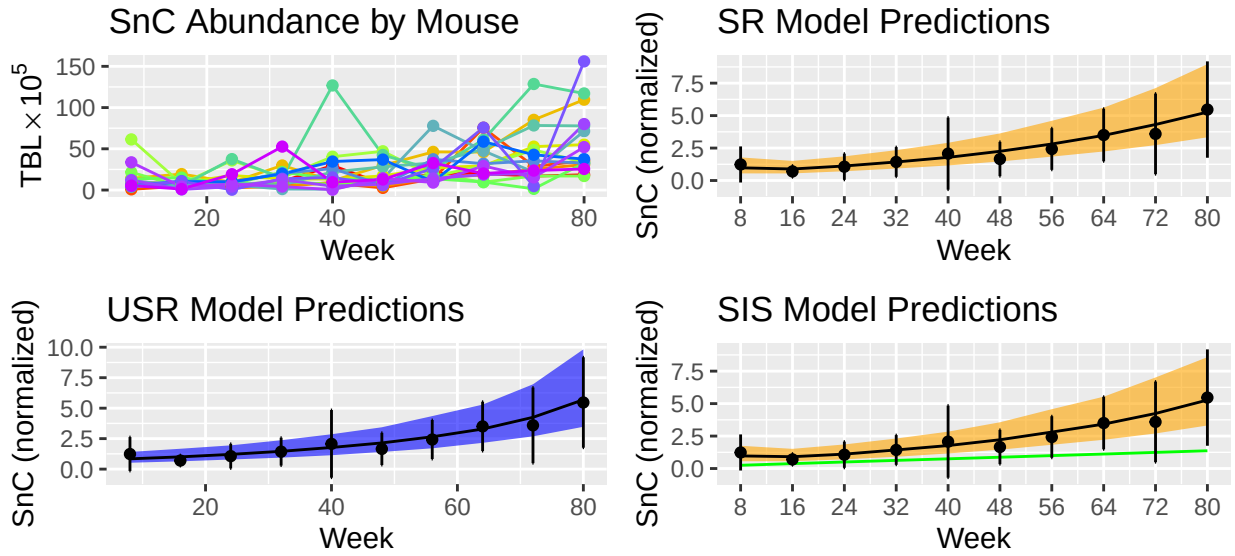

Figure 1: Unnormalized senescent cell (SnC) abundance trajectories for each mouse (top left). Retrodictions and 5%/95% credible intervals for SnC mean normalized abundance predicted by SR, USR, and SIS models (top right, bottom left, bottom right) respectively. Lines denote posterior median, dots denote observed mean abundance with error bars representing sample standard error. Green line in the SIS graph denotes estimated long-lived SnC abundance.

As a baseline for comparing our modified senescence-induced senescence model, we reproduced Karin et al. (2019)'s SR and USR models as Bayesian models in stan (Carpenter et al. 2017) (see Appendix 6.1 for details on priors, noise model, and stan configuration). At a high level, our results matched theirs. We compared the posterior probability of the two models and found that the SR model was 50.3 times more likely than the USR model (Gronau, Singmann, and Wagenmakers (2020)).

Although the SR model's full posterior fits the data meaningfully better than the USR model's, as Figure 1 shows, both models' credible intervals and posterior means mostly capture the observed data's evolution through time. This suggests that the maximum likelihood approach may have underestimated the quality of the USR model even if it correctly captures the superiority of the SR model.

2.3.1 Long-lived SnC senescence-induced senescence (SIS) model

As mentioned, the original full model included a term for SIS. However, the model treated SIS as growing as a function of overall SnC count and total SnC growth rate. Intuitively, given a long enough time this would inevitably lead to exponential growth of the number of senescent cells, which we don't observe. As suggested by Van Deursen (2014), it's instead possible that a small fraction of senescent cells both turn over more slowly and induce senescence in their neighbors, but the majority do not.

To test this hypothesis, we can modify[1]the SR model by replacing the current time-dependent growth rate term with a time-dependent long-lived cell SIS term:

$$\frac{\mathrm{dL}}{\mathrm{dt}} = \alpha \tag{2}$$

$$\frac{\mathrm{dC}}{\mathrm{dt}} = (\eta_0 + \eta_2 * L) - \frac{\beta_0 - \beta_1 * t}{1 + \beta_2 * C}. \tag{3}$$

In equation (3), $\frac{\mathrm{dL}}{\mathrm{dt}}$ denotes the time rate of change of (latent) long-lived senescent cell count. Solving for L this becomes

$$\frac{\mathrm{dC}}{\mathrm{dt}} = (\eta_0 + \eta_2 * l + \eta_2 * \alpha t) - \frac{\beta_0 - \beta_1 * t}{1 + \beta_2 * C} * C. \tag{4}$$

where l denotes the long-lived SnC abundance and αt the (assumed to be linear) increase as a function of time.

2.3.2 Modifications for pulse dataset

In order to compare models in a second regime, we fit variants of SR and SIS models on the pulse dataset. Given this dataset's small number of mice and time points (5 weeks in the young mice cohort, 2 weeks in the old mice cohort), we used our posterior estimates of parameters from the longitudinal model as priors for the corresponding parameters in the pulse models. We also removed the time-dependent term from the SIS model after finding it didn't contribute to the quality of the model's fit.

3 Results

3.1 Long-lived SnC SIS model fits the longitudinal dataset better than the base models

Our new long-lived SnC SIS model accurately describes the SnC growth dynamics of the longitudinal dataset. In fact, we find that it fits the data, as measured by both Bayes Factor and LOO-CV, better (under a uniform prior between models for the Bayes Factor) than the SR model (Bayes Factor of 25 and slightly higher ELPD-LOO). This suggests that long-lived senescent cell SIS may partially explain senescent cell dynamics when combined with saturated removal.

[1]As discussed in the appendix, we also remove the independent noise and instead model it as a noise-variance term in our likelihood.

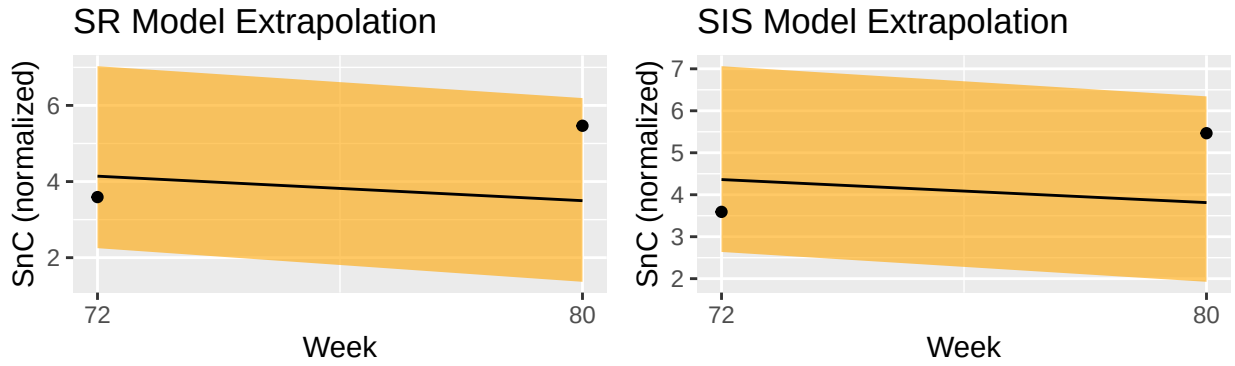

Figure 2: SR and SIS model predictive distributions for held-out weeks 72 and 80. As in Figure 1, dots denote true abundance values, lines predictive medians, and yellow bars 5%/95% predictive intervals. Both models incorrectly predict a slowdown in SnC growth but capture both points in their predictive distributions.

That said, when we compare this model's retrodictions of mean SnC count to the SR model's, we can see essentially no difference between the two (again see Figure 1). Given this, to try and further validate our claim that the SIS model is better, we tested the SR and SIS models' ability to extrapolate to held-out time steps. We split the SnC abundance observations into train and test set with the train set consisting of the first 7 weeks of abundance observations and the test set the final 3. Unfortunately, as 2 shows, neither model performed particularly well at extrapolation with both wrongly predicting a decline in SnC growth. Taking this poor performance on an absolute scale into account, we see that the SIS model slightly outperformed the SR model insofar as its upper error bar comes closer to correctly predicting the continued growth in SnC count. We hypothesize that this poor performance results from the final 2 weeks' worth of data playing an important role in helping the model learn the saturation points. This belief is bolstered by the fact that both the SR and SIS models trained on only the first 8 weeks of SnC abundance data learn higher saturation points than the corresponding full models but basically identical growth rates and long-lived SnC counts.

3.2 Long-lived SnC SIS model doesn't fit the pulse data as well as the SR model

Unlike with the longitudinal dataset, on the pulse dataset, the SIS model's increased complexity does not seem to improve the model's fit. As measured by Bayes Factor, the SR model is approximately twice as probable as the SIS model with respect to the pulse data. We admittedly didn't predict this before running the model. In retrospect, it can be partially explained by a combination of the pulse dataset having been generated in a way that likely would only increase the number of acute SnCs, not long-lived ones, and the long-lived cell SIS not contributing meaningful growth in the relatively short timescale of the pulse dataset. In spite of this justification, this finding should be taken as providing some, albeit weak evidence, against the long-lived SIS hypothesis.

3.3 SIS model estimates that long-lived SnCs comprise between 10% and 40% of all SnCs

Our model's median estimate for fraction of SnCs that are long-lived starts at 0.203 and grows to a final value of 0.25, with 5%/95% lower and upper bounds of 0.062/0.452 and 0.08/0.651. Keeping in mind that our model infers its parameters from a small, noisy dataset, this implies that long-lived SnCs could account for a meaningful fraction of all SnCs, with this fraction growing dramatically throughout the mouse lifespan.

4 Discussion

4.1 Strengths and Limitations

Our work has a few strengths. First, by using a fully Bayesian approach, we're better able to quantify our uncertainty about different parameter values. This directly enabled us to, for example, recognize that our SIS model put fairly wide bounds on the relative abundance of long-lived senescent cells. By employing stan and its suite of diagnostic tools, we were also better able to verify our model's fit and verify its parameter estimates satisfied various sanity checks. Finally, the Bayesian approach enables more sophisticated model comparison, which showed both the better fit of the SIS model on the longitudinal data and the marginally worse fit of it on the pulse data.

On the other hand, our work is limited by our datasets and our modeling assumptions. The longitudinal dataset we use has three major limitations:

1. It's relatively small, leading to wide error bars on our parameter estimates and also preventing us from accurately modeling inter-mouse heterogeneity.
2. It lacks spatial information, preventing us from testing whether SIS is mediated by cellular proximity.
3. Its time steps are coarse-grained relative to a mouse's lifespan, making extrapolation difficult.

The pulse dataset is even smaller than the longitudinal dataset and this made extracting useful additional information on parameter estimates from it a challenge, especially in the case of the old mouse cohort.

On the modeling side, our SIS model is partially unidentifiable because increases in η_2 can be partially compensated by decreases in α and vice versa. Fundamentally, this is necessary as long as the number of long-lived cells are latent but it complicates inference nonetheless.

4.2 Implications

While our results are not strong enough to enable a definitive conclusion regarding long-lived SnCs' role in shifting SnC growth dynamics, they suggest that the distinction between acute and long-lived SnCs warrants investigation in future experimental work. In particular, future data collection efforts that capture spatial proximity can help future modeling efforts better test the long-lived SnC SIS hypothesis.

More broadly, our success with applying a fully Bayesian approach to modeling SnC growth trajectory illustrates the power of the Bayesian approach for combining ODEs with robust uncertainty measurement. Relative to prior work, our work provides more robust uncertainty estimates for biologically relevant parameters and while enabling more principled model comparison.

5 Conclusion

We developed a fully Bayesian model of SnC growth dynamics and fit it on two datasets – a longitudinal SnC growth trajectory dataset and a SnC pulse dataset. We compared our model to Bayesian variants of Saturating Removal and Unsaturated Removal models proposed by Karin et al. (2019) and found that the SIS model fits the longitudinal dataset better than both the SR and USR models but does not fit the pulse dataset as well as the SR model, measured by both Bayes Factors and Leave-One-Out Cross-Validation. We then estimated the median fraction of long-lived SnCs in the longitudinal dataset and 5%-95% credible interval for that fraction. Our results are preliminary but suggest that long-lived SnC senescence-induced senescence is worth investigating as part of future experimental work.

6 Appendix

6.1 Differences between our and the original model

As mentioned in the main body, in order to reproduce Karin et al. (2019)'s model in the Bayesian framework and compare it to our SIS model, we had to change the model in a few ways.

6.1.1 Fully Bayesian vs. Maximum Likelihood model

The biggest change we made to the model, putting priors on parameters, falls out of our adoption of the Bayesian paradigm.

6.1.1.1 Priors We put weakly informative half-normal priors on all ODE parameters with prior hyperparameters either chosen based on stan's Prior Choice Recommendations or targeting a fraction of probability mass being within some range.

In all three models, η_0, β_0 we use $\mathcal{N}^+(0, .78$ priors to ensure that 99% of the prior probability mass for initial growth / removal rates is under 2. We chose 2 as the boundary because initial growth at this rate would imply a turnover rate strongly at odds with domain knowledge and the results of Karin et al. (2019).

For η_1, β_1 we $\mathcal{N}^+(0, 1)$ priors based on the Prior Choice Recommendations document.

In the SIS model, for α, following analogous logic to what we followed with η_0, β_0, we use a $(0, 0.025)$ prior, which puts 99% of the probability mass on values below 0.02. This is based on the assumption that long-lived SnCs shouldn't make up more than 60% of SnCs at week 50. For l, we use a HalfNormal$(0, .19)$ prior under the now familiar assumption that 99% of our probability mass should be on values below 99%. Again, this makes sense given that in young mice it would be incredibly surprising for long-lived SnCs to make up more than a relatively small fraction of all SnCs.

Finally, for our likelihood's standard deviation, we use a $\mathsf{LogNormal}(-1, 1)$ prior, following the multiplicative error model in Carpenter (2018).

6.1.1.2 Approximate Posterior Uncertainty (vs. Analytical Approximations) In Karin et al. (2019), they use analytical approximation to determine key uncertainty measures such as standard deviations of parameter estimates. Here, we instead leverage posterior simulation to estimate parameter uncertainty and generate retrodictions.

6.1.2 Normally-distributed error with ODE vs. stochastic differential equation

The original model includes independent error terms for each time step, with these error terms integrating to a Wiener process. Instead of time-specific error terms, we use a normal likelihood parameterized by the output of the integrated ODE at a given timestep and a single independent standard deviance parameter (with a $\text{Log} - \text{Normal}(-1, 1)$ prior).

6.1.3 Auto-catalysis term vs. SIS term

Karin et al. (2019) test a model that includes auto-catalysis, a different name for what we call senescence-induced senescence. However, they found that models that included auto-catalysis didn't fit the data as well as models that excluded. So why do our results differ from theirs? Although it's hard to be certain the degree to which this is a result of our use of a Bayesian approach vs. a maximum likelihood one, we believe our approach of explicitly modeling auto-catalysis as only being driven by a fraction of the SnC population also plays a role. Concretely, we suspect that including a separate term for initial long-lived SnC population enabled our model to better disentangle overall SnC growth and SIS-driven growth.

References

Burd, Christin E, Jessica A Sorrentino, Kelly S Clark, David B Darr, Janakiraman Krishnamurthy, Allison M Deal, Nabeel Bardeesy, Diego H Castrillon, David H Beach, and Norman E Sharpless. 2013. "Monitoring Tumorigenesis and Senescence in Vivo with a p16INK4a-Luciferase Model." *Cell* 152 (1-2): 340–51.

Campisi, Judith, and Fabrizio D'Adda Di Fagagna. 2007. "Cellular Senescence: When Bad Things Happen to Good Cells." *Nature Reviews Molecular Cell Biology* 8 (9): 729–40.

Carpenter, Bob. 2018. "Predator-Prey Population Dynamics: The Lotka-Volterra Model in Stan." *Pridobljeno S Https://Mc-Stan. Org/Users/Documentation/Case-Studies/Lotka-Volterra-Predator-Prey. Html [28. 8. 2019]* 62.

Carpenter, Bob, Andrew Gelman, Matthew D Hoffman, Daniel Lee, Ben Goodrich, Michael Betancourt, Marcus Brubaker, Jiqiang Guo, Peter Li, and Allen Riddell. 2017. "Stan: A Probabilistic Programming Language." *Journal of Statistical Software* 76 (1).

Gronau, Quentin F., Henrik Singmann, and Eric-Jan Wagenmakers. 2020. "bridgesampling: An R Package for Estimating Normalizing Constants." *Journal of Statistical Software* 92 (10): 1–29. https://doi.org/10.18637/jss.v092.i10.

He, Shenghui, and Norman E Sharpless. 2017. "Senescence in Health and Disease." *Cell* 169 (6): 1000–1011.

Karin, Omer, Amit Agrawal, Ziv Porat, Valery Krizhanovsky, and Uri Alon. 2019. "Senescent Cell Turnover Slows with Age Providing an Explanation for the Gompertz Law." *Nature Communications* 10 (1): 1–9.

Krtolica, Ana, Simona Parrinello, Stephen Lockett, Pierre-Yves Desprez, and Judith Campisi. 2001. "Senescent Fibroblasts Promote Epithelial Cell Growth and Tumorigenesis: A Link Between Cancer and Aging." *Proceedings of the National Academy of Sciences* 98 (21): 12072–7.

Nelson, Glyn, James Wordsworth, Chunfang Wang, Diana Jurk, Conor Lawless, Carmen Martin-Ruiz, and Thomas von Zglinicki. 2012. "A Senescent Cell Bystander Effect: Senescence-Induced Senescence." *Aging Cell* 11 (2): 345–49.

Ricón, José Luis. 2020. "Is Cellular Senescence Irreversible?" *Nintil*.

Van Deursen, Jan M. 2014. "The Role of Senescent Cells in Ageing." *Nature* 509 (7501): 439–46.

Yao, Yuling, Aki Vehtari, Daniel Simpson, and Andrew Gelman. 2017. "Using Stacking to Average Bayesian Predictive Distributions." *Bayesian Analysis*. https://doi.org/10.1214/17-BA1091.